

# UCLA

## UCLA Previously Published Works

### Title

Optical constants of silica glass from extreme ultraviolet to far infrared at near room temperature

### Permalink

<https://escholarship.org/uc/item/0st1d3tg>

### Journal

Applied Optics, 46(33)

### ISSN

0003-6935

### Authors

Kitamura, Rei  
Pilon, Laurent  
Jonasz, Miroslaw

### Publication Date

2007-11-01

Peer reviewed

# Optical Constants of Silica Glass From Extreme Ultraviolet to Far Infrared at Near Room Temperatures

Rei Kitamura, Laurent Pilon<sup>1</sup>

*Mechanical and Aerospace Engineering Department*

*Henry Samueli School of Engineering and Applied Science*

*University of California, Los Angeles - Los Angeles, CA 90095, USA*

*Phone: +1 (310)-206-5598, Fax: +1 (310)-206-2302*

*pilon@seas.ucla.edu*

Mirosław Jonasz

*MJC Optical Technology*

*217 Cadillac Street Beaconsfield, QC H9W 2W7, Canada*

This paper thoroughly and critically reviews studies reporting the real (refractive index) and imaginary (absorption index) parts of the complex refractive index of silica glass over the spectral range from 30 nm to 1,000  $\mu\text{m}$ . The general features of the optical constants over the electromagnetic spectrum are relatively consistent throughout the literature. In particular, silica glass is effectively opaque for wavelengths shorter than 200 nm and larger than 3.5-4.0  $\mu\text{m}$ . Strong absorption bands are observed (i) below 160 nm due to interaction with electrons, absorption by impurities, and the presence of OH groups and point defects, (ii) around 2.73-2.85  $\mu\text{m}$ , 3.5  $\mu\text{m}$ , and 4.3  $\mu\text{m}$  also caused by OH groups, (ii) around 9-9.5  $\mu\text{m}$ , 12.5  $\mu\text{m}$ , and 21-23  $\mu\text{m}$  due to Si-O-Si resonance modes of vibration. However, the actual values of the refractive and absorption indices can vary significantly due to the glass manufacturing process, crystallinity, wavelength, temperature, and to the presence of impurities, point defects, inclusions, and bubbles, as well as to the experimental uncertainties and approximations in the retrieval methods. Moreover, new formulas providing comprehensive approximations of the optical properties of silica glass are proposed between 7 and 50  $\mu\text{m}$ . These formulas are consistent with experimental data and substantially extend the spectral range of 0.21 to 7  $\mu\text{m}$  covered by existing formulas and can be used in various engineering applications. © 2007 Optical Society of America

*OCIS codes:* 160.6030, 160.4760, 290.3030, 160.4670, 050.5298, 110.5220

## 1. Introduction

Silicon dioxide ( $\text{SiO}_2$  or silica) has many forms including three main crystalline varieties: quartz, tridymite, and cristobalite.<sup>1,2</sup> Silica can also exist in non-crystalline form as silica glass or vitreous silica,<sup>1</sup> also referred to as amorphous silica and glassy silica. There are four basic types of commercial silica glasses:<sup>3,4</sup> (1) *Type I* is obtained by electric melting of natural quartz crystal in vacuum or in an inert gas at low pressure, (2) *Type II* is produced from quartz crystal powder by flame fusion, (3) *Type III* is synthetic and produced by hydrolyzation of  $\text{SiCl}_4$  when sprayed into an oxygen-hydrogen flame, and (4) *Type IV* is also synthetic and produced from  $\text{SiCl}_4$  in a water vapor-free plasma flame.

Each type of silica glasses has its own impurity level and optical properties. For example, *Type I* silica glasses tend to contain metallic impurities.<sup>3,4</sup> On the other hand, *Types III* and *IV* are much purer than *Type I* and feature greater ultraviolet transmission.<sup>3,4</sup> However, *Type III* silica glasses have, in general, higher water content, and infrared (IR) transmission is limited by strong water absorption peaks at wavelengths around 2.2 and 2.7  $\mu\text{m}$ .<sup>3-5</sup> *Type IV* is similar to *Type III* but contains less water and thus has better IR transmission. Suppliers provide various product grades for different optical applications.<sup>3,4,6</sup> Trade names of *Type I* silica glass are Infrasil, IR-Vitreosil, Pursil, and GE 105, for example. On the other hand, KU, Herosil, Homosil, Vitrasil, and O.G. Vitreosil are *Type II*. Moreover, KU-1, KV, Suprasil I, Tetrasil, Spectrosil,

and Corning 7940 are known as synthetic fused silica and classified as *Type III*. Finally, KI, Suprasil W, Spectrosil WF and Corning 7943 are *Type IV* silica glass. The term “fused quartz” is usually used for *Type I* and “fused silica” is used for synthetic fused silica, i.e., *Types III* or *IV*. In practice, however, those terms are often used interchangeably.

Because of its favorable physical, chemical, and optical characteristics, silica glass has been used in numerous applications: (1) as laboratory glassware, (2) in optics, as lenses or beam splitters, (3) for lighting and infrared heating, (4) in telecommunication, as fiber optics, (5) in micro and optoelectronics, as dielectric insulator, waveguide, photonic crystal fibers, or projection masks for photolithography, and (6) in thermal protection systems, as fibrous thermal insulation. In all these applications, optical properties are essential in predicting and optimizing the optical and thermal radiation performances of this material. Silica fiber optics, for example, are used in the near infrared around 1.31 and 1.55  $\mu\text{m}$  due to their low optical attenuation and optical dispersion.<sup>7,8</sup> In lens design, one often needs to fit and interpolate refractive index data which are reported or measured at discrete wavelengths over a certain spectral regions.<sup>9,10</sup> On the other hand, astronomers and atmospheric scientists are interested in optical properties of interstellar and atmospheric silica particles in the mid- and far-infrared region of the spectrum.<sup>11-13</sup>

The complex refractive index,  $m_\lambda$ , of silica glass at wavelength  $\lambda$  is defined as,

$$m_\lambda = n_\lambda + ik_\lambda \quad (1)$$

where  $n_\lambda$  is the refractive index and  $k_\lambda$  is the absorption index. The wavelength  $\lambda$  is related to other quantities such as frequency  $\nu$  and wavenumber  $\eta$  according to,

$$\lambda = \frac{c_\lambda}{\nu} = \frac{1}{\eta} \quad (2)$$

where  $c_\lambda$  is the speed of light at wavelength  $\lambda$  in vacuum. Therefore, the refractive and absorption indices can also be expressed as functions of frequency and denoted by  $n_\nu$  and  $k_\nu$ , or as functions of wavenumber and denoted by  $n_\eta$  and  $k_\eta$ .

The experimental data for the refractive and absorption indices vary in precision depending on the measurement techniques used and on the approximations made in retrieving the intrinsic optical properties. One should also keep in mind that these optical properties may be sensitive to the presence of impurities, crystallinity, point defects, inclusions, bubbles, wavelength, temperature, and the glass manufacturing process. In addition, when considering the literature it is often difficult to choose the set of experimental data or formula to use and to assess their validity. The objectives of this paper are (1) to critically review and compare the experimental data reported in the literature for the complex refractive index of silica glass and (2) to develop formulas that provide a comprehensive approximation of the measured data near room temperature. Given the wide range of engineering and scientific applications, the spectral range from 30 nm to 1,000  $\mu\text{m}$  is considered.

## 2. Experimental Methods

### 2.A. Refractive Index, $n_\lambda$

Various experimental techniques and procedures have been used to retrieve the real part of the complex refractive index  $n_\lambda$ . The most accurate is the minimum deviation angle method<sup>14</sup> which relies on measuring the minimum deviation angle  $\theta_{min}$  of an isosceles triangular prism made of the silica glass placed in air. This method is based on Snell's law<sup>14</sup> and the refractive index  $n_\lambda$  can be estimated by,

$$n_\lambda = \frac{\sin\left(\frac{\theta_{min} + \phi}{2}\right)}{\sin\left(\frac{\phi}{2}\right)} n_{air} \quad (3)$$

where  $\phi$  is an apex angle of the prism sample and  $n_{air}$  is the refractive index of air ( $n_{air} = 1$ ). This method is often used to accurately measure the refractive index of highly transparent glass for which the absorption index  $k_\lambda$ , i.e., the imaginary part of the complex refractive index, is negligibly small.

Alternatively, the interferometric method is also used to measure  $n_\lambda$ . It is based on observing the interference fringes created when light is incident normally upon a silica glass plate.<sup>15,16</sup> Other techniques include the Abbe's or the Pulfrich's refractometers whose accuracy on the index of refraction is within  $\pm 2 \times 10^{-3}$  and  $\pm 5 \times 10^{-5}$ , respectively.<sup>17</sup>

Moreover, when absorption cannot be ignored, both  $n_\lambda$  and  $k_\lambda$  can be retrieved from the directional or hemispherical reflectance and/or emittance of a slab of known thickness. Electromagnetic wave theory can be used to retrieve both  $n_\lambda$  and  $k_\lambda$  assuming

optically smooth surfaces and accounting for internal reflection.<sup>18</sup>

Finally, the Kramer-Krönig relations<sup>18</sup> can also be used to predict either the refractive index from the absorption index, or vice-versa at frequency  $\nu$ .<sup>18,19</sup>

$$n_\nu = 1 + \frac{2}{\pi} P \int_0^\infty \frac{\nu' k_{\nu'}}{\nu'^2 - \nu^2} d\nu' \quad (4)$$

$$k_\nu = \frac{-2\nu}{\pi} P \int_0^\infty \frac{n_{\nu'}}{\nu'^2 - \nu^2} d\nu' \quad (5)$$

where P denotes the Cauchy principle value of the integral.<sup>18</sup>

Alternatively, the refractive and absorption indices can be simultaneously obtained from reflectance. First, the phase angle of the complex reflection coefficient  $\Theta$ , at frequency  $\nu_0$  can be expressed by the Kramer-Krönig relations,<sup>20</sup>

$$\Theta(\nu) = \frac{2\nu}{\pi} P \int_0^\infty \frac{\ln R(\nu')}{\nu'^2 - \nu^2} d\nu' \quad (6)$$

where  $R(\nu)$  is the normal-normal reflectivity expressed as a function of  $\nu$

$$R(\nu) = |r|^2 = \frac{(n_\nu - 1)^2 + k_\nu^2}{(n_\nu + 1)^2 + k_\nu^2} \quad (7)$$

The Fresnel reflection coefficient  $r$  is defined as,

$$r = \frac{1 - n_\nu - ik_\nu}{1 + n_\nu + ik_\nu} = |r|e^{i\Theta} \quad (8)$$

From Equations (7) and (8), the refractive and absorption indices can be expressed as,

$$n_\nu = \frac{1 - R(\nu)}{1 + R(\nu) - 2\sqrt{R(\nu)} \cos \Theta} \quad (9)$$

$$k_\nu = \frac{-2\sqrt{R(\nu)} \sin \Theta}{1 + R(\nu) - 2\sqrt{R(\nu)} \cos \Theta} \quad (10)$$

However, due to the infinite bound of the integrals in Equations (4) to (6), these techniques require extrapolations into spectral regions where data is not always available. Furthermore, the integrals need to be computed numerically. Practical limitations and possible errors of Kramers-Krönig relations have been discussed by Riu and Lapaz.<sup>19</sup> These authors concluded that the Kramers-Krönig relations were practically applicable in almost every experimental situation.

### 2.B. Absorption Index, $k_\lambda$

The value of the absorption index  $k_\lambda$  was not always directly available from the literature and was sometimes recovered from the normal spectral transmittance or emittance data. Indeed, the value of  $k_\lambda$  can be recovered from the normal spectral transmittance  $T_{0,\lambda}$ , accounting for multiple reflections and expressed as,<sup>21</sup>

$$T_{0,\lambda}(L) = \frac{(1 - \rho_\lambda)^2 e^{-\kappa_\lambda L}}{1 - (\rho_\lambda)^2 e^{-2\kappa_\lambda L}} \quad (11)$$

where  $L$  is the thickness of the sample,  $\rho_\lambda$ , and  $\kappa_\lambda$  are the spectral reflectivity of the interface and the spectral absorption coefficient of silica glass, respectively, and are given by

$$\rho_\lambda = \frac{(n_\lambda - 1)^2 + k_\lambda^2}{(n_\lambda + 1)^2 + k_\lambda^2} \quad (12)$$

$$\text{and} \quad \kappa_\lambda = \frac{4\pi k_\lambda}{\lambda} \quad (13)$$

Equations (11) to (13) can be solved as a quadratic in the exponential factor in terms of  $k_\lambda$ . After some algebraic manipulation, one obtains the following expression for  $k_\lambda$  as a function of the refractive index,  $n_\lambda$ , the sample thickness,  $L$ , and the spectral normal transmittance,  $T_{0,\lambda}$ ,

$$k_\lambda = - \left( \frac{\lambda}{4\pi L} \right) \ln \left[ \frac{\sqrt{(1 - \rho_\lambda)^4 + 4\rho_\lambda^2 T_{0,\lambda}} - (1 - \rho_\lambda)}{2\rho_\lambda^2 T_{0,\lambda}} \right] \quad (14)$$

Alternatively, the absorption index,  $k_\lambda$ , can also be determined from measurements of the spectral normal emittance,  $\epsilon_{\lambda,0}$ , by using the following expression,<sup>22</sup>

$$k_\lambda = \left( \frac{\lambda}{4\pi L} \right) \ln \left[ \frac{1 - \rho_\lambda - \rho_\lambda \epsilon_{\lambda,0}}{1 - \rho_\lambda - \epsilon_{\lambda,0}} \right] \quad (15)$$

Note that the above expressions for the absorption index  $k_\lambda$  given by Equations (14) and (15) are valid if both  $(n_\lambda - 1)$  and  $(n_\lambda + 1)$  are much larger than  $k_\lambda$ . In either case, an expression for  $n_\lambda$  is necessary to estimate  $\rho_\lambda$ . As discussed later in this paper, the Sellmeier equation proposed by Malitson<sup>23</sup> can be used for that purpose between 0.21 and 6.7  $\mu\text{m}$ .

In addition, in the ultraviolet (UV) and infrared (IR) regions of the spectrum when silica glass is strongly absorbing, most reported value of  $n_\lambda$  and  $k_\lambda$  were retrieved from near-normal reflectance measurements in combination with the Kramer-Krönig relations.<sup>24</sup>

### 3. Experimental Data and Discussion

Table 1 summarizes representative references reporting experimental values of the complex refractive index of silica glass at room temperature for the spectral range from 30 nm and 1000  $\mu\text{m}$ . For each study, the measurement method, the spectral range, as well as the sample thicknesses, compositions, and temperatures investigated are also reported when available. In addition, the absorption index  $k_\lambda$  was derived from transmittance measurements using Equation (14) if it was not directly reported. Then, computation from transmittance and emittance data sometimes lead to negative values, particularly in the spectral region from 0.2 to 4.0  $\mu\text{m}$  where silica glass is very weakly absorbing. This was the case for transmittance data from references<sup>25</sup> and.<sup>26</sup> Hence, in this region, the experimental data should be used with care since the uncertainty for  $k_\lambda$  is very large and  $k_\lambda$  effectively vanishes.

Figure 1 shows the real and imaginary parts of the refractive index of silica glass,  $n_\lambda$  and  $k_\lambda$ , as a function of wavelength  $\lambda$  over the spectral range from 30 nm to 1,000  $\mu\text{m}$  as reported in the references listed in Table 1. Because of the density of data points in some part of the spectrum and for the sake of clarity, Figures 2 to 5 show details of both the real  $n_\lambda$  and imaginary  $k_\lambda$  parts of the complex index of refraction of silica glass for wavelengths between 30 nm and 1  $\mu\text{m}$ , 1  $\mu\text{m}$  and 15  $\mu\text{m}$ , 15  $\mu\text{m}$  and 100  $\mu\text{m}$ , and 100  $\mu\text{m}$  and 1000  $\mu\text{m}$ , respectively.

Overall, the reported values for both the real and imaginary parts of the complex

index of refraction agree relatively well. Studies showing large deviations from other studies suggest that the data is unreliable.<sup>24</sup> For example, data reported by Ellis *et al.*<sup>27</sup> strongly disagree with all other data between 60 nm and the visible. Locations of extrema of  $n_\lambda$  are consistent among all experimental data except for those reported by Tan<sup>28</sup> ( $7.19 \mu\text{ m} \leq \lambda \leq 9.06 \mu\text{ m}$ ), Khashan and Nassif<sup>29</sup> ( $0.2 \mu\text{ m} \leq \lambda \leq 3.0 \mu\text{ m}$ ), and Reitzel<sup>30</sup> ( $16.7 \mu\text{ m} \leq \lambda \leq 25 \mu\text{ m}$ ). The data for wavelengths below  $9 \mu\text{ m}$  as reported by various authors agree well with one another. However, the data agree considerably less for wavelengths between 9 and  $50 \mu\text{ m}$ . Beyond  $50 \mu\text{ m}$ , a smaller number of values for  $n_\lambda$  have been reported but the data agree relatively well.

Furthermore, trends and the locations of extrema in the measured absorption index are consistent from one study to another. However, discrepancies larger than those for  $n_\lambda$  can be observed in reported data for  $k_\lambda$  in some parts of the spectrum. They are most likely due to (i) the impurity of the sample (e.g., OH group, alkali, metallic content), (ii) the presence of inclusions, bubbles, or point defects, (iii) the sample preparation and surface optical quality, and/or (iv) the uncertainty in the measurement and retrieval techniques. Note that the flatness of the sample surface becomes a critical parameter in the visible and UV.<sup>31,32</sup> In this wavelength range, the surface roughness must remain much smaller than the wavelength to avoid surface scattering and consider the surface as optically smooth.

The imaginary part of the complex refractive index of silica glass  $k_\lambda$  is small from the near UV to the near-infrared part of the spectrum. Practically, silica glass is

transparent from 200 nm up to 3.5-4.0  $\mu\text{m}$ . In the extreme ultraviolet (for wavelengths below 200 nm) and in the infrared and far infrared (beyond 4.0) silica glass can be considered opaque. In the ultraviolet region of the spectrum below 200 nm, the strong absorption of silica glass is caused by interaction of the electromagnetic radiation with electrons of Si-O bonds<sup>17</sup> and with structural imperfections or point defects such as OH groups, Si-Si bonds, and strained Si-O-Si bonds.<sup>33</sup> This results in sharp UV cut-off (also called absorption edge) around 160 nm.<sup>17,34</sup> The location of the absorption edge depends on the glass composition, impurity level, and point defects formed during the manufacturing process<sup>17,33</sup> as well as on temperature.<sup>35</sup> For example, it is shifted towards the visible wavelengths due to the presence of impurities in particular ions  $\text{Fe}^{3+}$ ,  $\text{Cr}^{3+}$ , and  $\text{Ti}^{3+}$ .<sup>36</sup> Similar effects are observed when increasing the alkali contents<sup>34</sup> or the temperature.<sup>35</sup> On the contrary, the absorption edge is slightly shifted to lower wavelengths for crystal quartz.<sup>34</sup> Shifting the absorption edge to lower wavelengths (even slightly) has been the subject of intense studies to enable the use of silica glass for photomask material in 157-nm photolithography using  $\text{F}_2$  excimer lasers.<sup>32,37,38</sup> Acceptable transmittance around 157 nm has been achieved by minimizing the OH content of silica<sup>37</sup> or by doping silica glass with network modifiers such as fluorine which relaxes the glass structure and eliminates strained Si-O-Si bonds.<sup>33</sup> Experimental measurements and theoretical calculations of the electronic structure of  $\text{SiO}_2$  has been reviewed by Griscom<sup>39</sup> and spectroscopic data for wavelengths between 90 and 350 nm have been discussed by Sigel.<sup>34</sup> Interaction between

UV radiation and electrons and point defects is also responsible for the steep increase of  $n_\lambda$  for wavelengths less than 300 nm.

In the infrared part of the spectrum, silica glass is effectively opaque for wavelength larger than 3.5-4.0  $\mu\text{m}$ . Beyond this wavelength, three major absorption bands can be observed (Figure 1) due to resonance of Si-O-Si vibrations. The absorption peak between 9.0 and 9.5  $\mu\text{m}$  can be attributed to the asymmetric stretching vibration of Si-O-Si bridge.<sup>17,24</sup> The absorption band around 12.5  $\mu\text{m}$  is due to symmetric vibration stretching of Si-O-Si bridge involving the displacement of the oxygen atom perpendicular to the Si-Si direction in the Si-O-Si plane.<sup>24</sup> The third band between 21 and 23  $\mu\text{m}$  is the consequence of O-Si-O bending vibration but has also been attributed to the “rocking” mode of Si-O-Si bonds caused by the displacement of oxygen atom out of the Si-O-Si plane.<sup>24</sup> Resonance of Si-O-Si vibrations are also responsible for the sharp decreases in  $n_\lambda$  around the resonance wavelengths.<sup>17</sup> The reader is referred to Ref.<sup>24</sup> (pp.63-77) for detailed discussion on vibrational spectroscopy of silica glass at the above wavelengths. Moreover, smaller absorption bands around wavelengths 2.73-2.85  $\mu\text{m}$ , 3.5  $\mu\text{m}$ , 4.3  $\mu\text{m}$  correspond to the presence of OH groups in the structure of the glass.<sup>17,40-42</sup> The magnitude of the absorption depends on the melting technology and in particular on the partial pressure of water vapor above the melt during the melting process.<sup>17</sup> The concentration of OH groups in silica glass can be computed from the absorption band around wavelength 2.73-2.85  $\mu\text{m}$ .<sup>17</sup>

To the best of our knowledge, no model or approximate equation have been pro-

posed for the absorption index of silica glass. This is the subject of the next section.

#### 4. Optical Constant Theory

The complex index of refraction,  $m_\lambda = n_\lambda + ik_\lambda$ , and the complex relative dielectric permittivity,  $\epsilon(\lambda) = \epsilon'(\lambda) + i\epsilon''(\lambda)$  are related by the expression  $\epsilon(\lambda) = m_\lambda^2$ , i.e.,<sup>21</sup>

$$\epsilon'(\lambda) = n_\lambda^2 - k_\lambda^2 \quad \text{and} \quad \epsilon''(\lambda) = 2n_\lambda k_\lambda \quad (16)$$

Numerous physical models such as the Lorentz model, the Drude model, and the Debye relaxation model have been proposed to predict the optical properties of solids.<sup>18</sup>

The Lorentz model assumes that electrons and ions in the material are harmonic oscillators subject to the force applied by a time-dependent electromagnetic fields. Then the complex relative dielectric permittivity can be expressed in terms of frequency  $\nu$  as follows,<sup>21</sup>

$$\epsilon(\nu) = 1 + \sum_j \frac{\nu_{pj}^2}{\nu_j^2 - \nu^2 - i\gamma_j\nu} = 1 + \sum_j \frac{\nu_{pj}^2(\nu_j^2 - \nu^2) + i\gamma_j\nu_{pj}^2\nu}{(\nu_j^2 - \nu^2)^2 + \gamma_j^2\nu^2} \quad (17)$$

where  $\nu_{pj}$  and  $\nu_j$  are the plasma and resonance frequencies, respectively. The parameter  $\gamma_j$  is the damping factor of the oscillators. Only when  $\nu$  is very close to one of the resonance frequencies  $\nu_j$ , the imaginary terms in Equation (17) are important.<sup>43</sup>

Thus,  $\gamma_j\nu$  are negligibly small compared with  $(\nu_j^2 - \nu^2)$  for silica glass for wavelength below 7  $\mu\text{m}$  and  $\epsilon''$  is virtually equal to 0.0. Hence, after substituting Equation (2) into Equation (17),  $\epsilon$  can be expressed in terms of  $\lambda$  as follows,

$$\epsilon(\lambda) = \epsilon'(\lambda) = 1 + \sum_j \frac{A_j^2\lambda^2}{(\lambda^2 - \lambda_j^2)} \quad (18)$$

where  $A_j = \nu_{pj}\lambda_j/c_\lambda$  with  $\lambda_j$  being the resonance wavelength. Moreover, as  $\epsilon''(\lambda)$  vanishes, the medium is weakly absorbing and  $k_\lambda$  is negligibly small compared with  $n_\lambda$ . Then  $\epsilon'(\lambda)$  is equal to  $n_\lambda^2$  and given by the Sellmeier dispersion formula,

$$\epsilon'(\lambda) = n_\lambda^2 = 1 + \sum_j \frac{A_j^2 \lambda^2}{(\lambda^2 - \lambda_j^2)} \quad (19)$$

Different formulas for the refractive index of silica glass as a function of wavelength and based on the Sellmeier dispersion formula have been proposed in the literature<sup>23,44,45</sup> for different spectral regions. Rodney and Spindler<sup>44</sup> suggested a formula for  $n_\lambda$  over a spectral range from 0.347 to 3.508  $\mu\text{m}$  at 31°C while Tan and Arndt<sup>45</sup> proposed another equation in the spectral region from 1.44 to 4.77  $\mu\text{m}$  at temperatures ranging from 23.5 to 481°C. In addition, for the spectral range from 0.21 to 3.71  $\mu\text{m}$  at 20°C, Malitson<sup>23</sup> fitted experimental data with the following three-term Sellmeier equation,

$$n_\lambda^2 = 1 + \frac{0.6961663\lambda^2}{\lambda^2 - (0.0684043)^2} + \frac{0.4079426\lambda^2}{\lambda^2 - (0.1162414)^2} + \frac{0.8974794\lambda^2}{\lambda^2 - (9.896161)^2} \quad (20)$$

Tan<sup>16</sup> confirmed the validity of Equation (20) for wavelengths up to 6.7  $\mu\text{m}$ . Furthermore, for a spectral range over 8  $\mu\text{m}$ , an approximate piecewise linear fit was given by Dombrovsky.<sup>46</sup> However, no physics-based formulas have been developed for the spectral range beyond 8  $\mu\text{m}$ .

In parts of the spectrum where  $k_\lambda$  cannot be neglected or when the frequency  $\nu$  is very close to the resonance frequencies, the Sellmeier equation for  $n_\lambda$  is no longer valid and an alternative model must be used. Recently, Meneses *et al.*<sup>47</sup> proposed a new

dielectric function model based on the causal version of the Voigt function. The model was validated by fitting the infrared spectra of two difference glasses and confirmed to be more appropriate than the Lorentz model.<sup>47</sup> Moreover, the authors proposed another simplified model based on Gaussian functions.<sup>48</sup> Then, the dielectric constant can be written as,

$$\epsilon(\eta) = \epsilon'(\eta) + i\epsilon''(\eta) = \epsilon_\infty + \sum_j \left[ g_{cj}^{kkg}(\eta) + ig_{cj}(\eta) \right] \quad (21)$$

where the high frequency dielectric constant is denoted by  $\epsilon_\infty$ . In addition, the Gaussian functions  $g_{cj}(\eta)$  and  $g_{cj}^{kkg}(\eta)$  are defined as,

$$g_{cj}(\eta) = \alpha_j \exp \left[ -4 \ln 2 \left( \frac{\eta - \eta_{0j}}{\sigma_j} \right)^2 \right] - \alpha_j \exp \left[ -4 \ln 2 \left( \frac{\eta + \eta_{0j}}{\sigma_j} \right)^2 \right] \quad (22)$$

$$g_{cj}^{kkg}(\eta) = \frac{2\alpha_j}{\pi} \left[ D \left( 2\sqrt{\ln 2} \frac{\eta + \eta_{0j}}{\sigma_j} \right) - D \left( 2\sqrt{\ln 2} \frac{\eta - \eta_{0j}}{\sigma_j} \right) \right] \quad (23)$$

Here,  $\alpha_j$  is the amplitude,  $\eta_{0j}$  is the peak position,  $\sigma_j$  is the full width at half maximum, and  $D(x)$  is an operator defined as,

$$D(x) = e^{-x^2} \int_0^x e^{t^2} dt \quad (24)$$

In the present study, this model is used to interpolate the refractive index  $n_\lambda$  and absorption index  $k_\lambda$  for wavelengths  $\lambda$  between 7 and 50  $\mu\text{m}$ . It enables one to describe the experimental data with a reduced set of parameters<sup>48</sup> over a wide spectral range, including the spectral range where  $k_\lambda$  may be large. Note that the above simplified model satisfies the Kramers-Krönig relation.

The practical procedure for fitting complex refractive index data conducted in this paper is as follows: (i) the spectral reflectivity at normal incidence,  $R(\eta)$ , is computed from Equation (7), (ii) parameters of  $\epsilon(\eta)$  in Equations (21) to (22) are determined by curve fitting for  $R(\eta)$  expressed as,

$$R(\eta) = \left| \frac{\sqrt{\epsilon(\eta)} - 1}{\sqrt{\epsilon(\eta)} + 1} \right|^2 \quad (25)$$

and (iii)  $n_\eta$  and  $k_\eta$  are computed using Equation (16). The advantage of this procedure is that (a) fitting the reflectivity is easier than fitting  $n_\lambda$  and  $k_\lambda$  independently, (b) both  $n_\lambda$  and  $k_\lambda$  can be derived from a single curve fitting, and (c) the result automatically satisfies the Kramers-Krönig relations.

The experimental data of Popova *et al.*<sup>49</sup> were selected to develop formulas for both  $n_\lambda$  and  $k_\lambda$  because these data cover a wide spectral range from 7 to 50  $\mu\text{m}$ , and both the refractive and absorption indices are reported at the same wavelength enabling the calculation of  $R(\eta)$ . In the spectral region from 0.2 to 7  $\mu\text{m}$ , the absorption index of silica glass is very small and may be assumed to be zero for all practical purposes as suggested by Figure 1. Moreover, reported data, including that of Popova *et al.*,<sup>49</sup> indicates that the refractive index is satisfactorily predicted by the Sellmeier formula reported by Maliston<sup>16,23</sup> between 0.2 and 7  $\mu\text{m}$  and given by Equation (20). Therefore, the present study focuses on the spectral range between 7 and 50  $\mu\text{m}$ .

In order to fit the model with experimental data, the FOCUS software was used.<sup>47,48</sup> By adding terms in Equation (21) one by one, eight terms were found to best fit the

experimental data. The fitting curves obtained in this study are shown in Figures 3 and 4, and the associated parameters  $\alpha_j$ ,  $\eta_{0j}$ , and  $\sigma_j$  used in Equations (21) to (22) are summarized in Table 2. The fitting curves for  $n_\lambda$  and  $k_\lambda$  obtained in the present study agree well with the data of Popova *et al.*,<sup>49</sup> and with most of other data shown in Figures 3 and 4. The differences (or residuals) between the data of Popova *et al.*<sup>49</sup> and the model predictions for both  $n_\lambda$  and  $k_\lambda$  using the parameters given in Table 2 are shown in Figure 6. It indicates that the residuals are less than 0.06 except around 9 and 22.5  $\mu\text{m}$  where they reach up to 0.3 around 9  $\mu\text{m}$  and 0.14 around 22.5  $\mu\text{m}$ . This can be attributed to the fact that the refractive index changes greatly in those wavelength region. However, these residuals errors are small compared with much larger differences observed in the experimental data reported for  $n_\lambda$ . For example, one can see differences larger than 0.5 among reported refractive index data in the spectral range between 9 and 10  $\mu\text{m}$ . Thus, the approximation obtained here is acceptable and can be useful in engineering applications.

Moreover, the residuals between the experimental data for the refractive and absorption indices listed in Table 1 and the model predictions using the parameters given in Table 2 are shown in Figure 7. Here again, the residuals are less than 0.3 except around 9.0 and 22.5  $\mu\text{m}$ . This indicates that the model predictions using the parameters given in Table 2 agree with all data reported in the literature at the spectral range except around 9 and 22.5  $\mu\text{m}$ . However, large discrepancies in reported experimental data sets can be observed around these two wavelengths. In general, the

model should be used with care when applied outside the spectral range from 0.2 to 50  $\mu\text{m}$  of interest for most applications.

Finally, given its widespread use, particular attention was paid to the compilation of data reported by Philipp<sup>50</sup> for the refraction and absorption indices of silica glass over the spectral range from 0.006 to 500  $\mu\text{m}$ . The compilation consists of experimental data reported by various authors<sup>15,20,51-54</sup> as well as unpublished data. Philipp<sup>50</sup> also retrieved optical properties from absorption coefficient as well as computer generated values. Qualitatively, good agreement between data compiled by Philipp<sup>50</sup> and other data is observed in Figs. 2 through 5. Moreover, residual with the present model range from -0.42 to 0.19 for  $n_\lambda$  and -0.25 to 0.37 for  $k_\lambda$  from 7 to 50  $\mu\text{m}$ .

## 5. Conclusions

A thorough review of experimental data for the complex refractive index of silica glass at near room temperatures over a spectral range from 30 nm to 1000  $\mu\text{m}$  implies that the values reported in the literature can vary significantly due to numerous sample features and experimental methods and conditions. Hence, it is essential to report the silica glass synthesis method, composition, impurity and defects level, sample thickness, surface roughness, and temperatures as well as the retrieval method and the underlying assumptions when one reports optical properties of glass. However, the general features of the complex refractive index spectra are relatively consistent throughout the region of the spectrum considered. Silica glass is effectively opaque

for wavelengths shorter than 200 nm and larger than 3.5-4.0  $\mu\text{m}$ . Strong absorption bands are observed (i) below 160 nm due to interaction with electrons, absorption by impurities, and the presence of OH groups and point defects, (ii) around 2.73-2.85  $\mu\text{m}$ , 3.5  $\mu\text{m}$ , and 4.3  $\mu\text{m}$  also caused by OH groups, (iii) around 9-9.5  $\mu\text{m}$ , 12.5  $\mu\text{m}$ , and 21-23  $\mu\text{m}$  due to Si-O-Si resonance modes of vibration. New formulas for both the real and imaginary parts of the complex refractive index are proposed over a wide spectral range between 7 and 50  $\mu\text{m}$  thus, complementing the existing analytical formula for  $n_\lambda$  in the range of 0.21 to 7  $\mu\text{m}$ .<sup>16,23</sup> The imaginary part of the complex refractive index can be neglected in much of this range (0.21 to 4  $\mu\text{m}$ ). The differences between various experimental data are comparable and greater than the differences between the results of these formulas and the experimental data used to develop them. Hence it is believed that the formulas proposed are useful for practical engineering applications such as simulations and optimizations of optical and thermal systems. The data collected and presented in this study are available in digital form online<sup>55</sup> or directly from the corresponding author upon request.

### **Acknowledgment**

The authors would like to thank Asahi Glass Co., Ltd. Japan for financial support. They are grateful to Dr. D. De Sousa Meneses for helpful discussion about FOCUS. The contribution of M. Jonasz was supported by MJC Optical Technology.

## References

1. G. Hart, "The nomenclature of silica," *American Mineralogist* **12**, 383–395 (1927).
2. R. B. Sosman, *The Phase of Silica* (Rutgers University Press, New Brunswick, NJ, 1964).
3. G. Hetherington, K. H. Jack, and M. W. Ramsay, "The high-temperature electrolysis of vitreous silica, Part I. Oxidation, ultra-violet induced fluorescence, and irradiation colour," *Physics and Chemistry of Glasses* **6**, 6–15 (1965).
4. R. Bruckner, "Properties and structure of vitreous silica. I," *Journal of Non-Crystalline Solids* **5**, 123–175 (1970).
5. K. M. Davis, A. Agarwal, M. Tomozawa, and K. Hirao, "Quantitative infrared spectroscopic measurement of hydroxyl concentrations in silica glass," *Journal of Non-Crystalline Solids* **203**, 27–36 (1996).
6. R. H. Doremus, *Glass Science* (John Wiley & Sons, New York, NY, 1994).
7. J. M. Senior, *Optical Fiber Communications : Principles and Practice, 2nd edition* (Prentice Hall, Upper Saddle River, NJ, 1992).
8. G. E. Keiser, *Optical Fiber Communications, 3<sup>rd</sup> Edition* (McGraw Hill Higher Education - International Editions: Electrical Engineering Series, New York, NY, 2000).
9. B. Brixner, "Refractive-index interpolation for fused silica," *Journal of Optical Society of America* **57**, 674–676 (1967).

10. L. E. Sutton and O. N. Stavroudis, "Fitting refractive index data by least squares," *Journal of the Optical Society of America* **51**, 901–905 (1961).
11. T. Steyer, K. L. Day, and R. Huffman, "Infrared absorption by small amorphous quartz spheres," *Applied Optics* **13**, 1586–1590 (1974).
12. T. Henning and H. Mutschke, "Low-temperature infrared properties of cosmic dust analogues," *Astronomy and Astrophysics* **327**, 743–754 (1997).
13. C. Koike, H. Hasesgawa, N. Asada, and T. Komatuzaki, "Optical constants of fine particles for the infrared region," *Monthly Notices of the Royal Astronomical Society* **239**, 127–137 (1989).
14. M. Born and E. Wolf, *Principles of Optics, 7<sup>th</sup> Edition* (Cambridge University Press, Cambridge, UK, 1999).
15. C. M. Randall and R. D. Rawcliffe, "Refractive indices of germanium, silicon, and fused quartz in the far infrared," *Applied Optics* **6**(11), 1889–1895 (1967).
16. C. Tan, "Determination of refractive index of silica glass for infrared wavelengths by IR spectroscopy," *Journal of Non-Crystalline Solids* **223**, 158–163 (1998).
17. I. Fanderlik, *Glass Science and Technology, Vol. 5: Optical Properties of Glass* (Elsevier Science, New York, NY, 1983).
18. C. F. Bohren and D. R. Huffman, *Absorption and Scattering of Light by Small Particles* (John Wiley & Sons, New York, NY, 1983).
19. P. J. Riu and C. Lapaz, "Practical limits of the Kramers-Krönig relationships

- applied to experimental bioimpedance data,” *Annals of the New York Academy of Sciences* **873**, 374–380 (1999).
20. H. Philipp, “The infrared optical properties of SiO<sub>2</sub> and SiO<sub>2</sub> layers on silicon,” *Journal of Applied Physics* **50**, 1053–1057 (1979).
  21. M. F. Modest, *Radiative Heat Transfer* (Academic Press, San Diego, CA, 2003).
  22. A. V. Dvurechensky, V. Petrov, and V. Y. Reznik, “Spectral emissivity and absorption coefficient of silica glass at extremely high temperatures in the semi-transparent region,” *Infrared Physics* **19**, 465–469 (1979).
  23. I. Malitson, “Interspecimen comparison of the refractive index of fused silica,” *Journal of the Optical Society of America* **55**, 1205–1209 (1965).
  24. A. M. Efimov, *Optical Constants of Inorganic Glasses* (CRC Press Inc., Boca Raton, FL, 1995).
  25. L. Bogdan, “Measurement of radiative heat transfer with thin-film resistance thermometers,” NASA-CR-27 pp. 1–39 (1964).
  26. A. Sviridova and N. Suikovskaya, “Transparent limits of interference films of Hafnium and Thorium oxides in the ultraviolet region of the spectrum,” *Optics and Spectroscopy* **22**, 509–512 (1967).
  27. E. Ellis, D. W. Johnson, A. Breeze, P. M. Magee, and P. G. Perkins, “The electronic structure and optical properties of oxide glasses I. SiO<sub>2</sub>, Na<sub>2</sub>O:SiO<sub>2</sub> and Na<sub>2</sub>O:CaO:SiO<sub>2</sub>,” *Philosophical Magazine B* **40**(2), 105–124 (1979).

28. C. Tan, "Optical interference and refractive index of silica glass in the infrared absorption region," *Journal of Non-Crystalline Solids* **249**, 51–54 (1999).
29. M. Khashan and A. Nassif, "Dispersion of the optical constants of quartz and polymethyl methacrylate glasses in a wide spectral range: 0.2-3  $\mu\text{m}$ ," *Optics Communications* **188**, 129–139 (2001).
30. J. Reitzel, "Infrared spectra of  $\text{SiO}_2$  from 400  $\text{cm}^{-1}$  to 600  $\text{cm}^{-1}$ ," *Journal of Chemical Physics* **23**, 2407–2409 (1955).
31. G. M. Mansurov, R. K. Mamedov, S. Sudarushkin, V. K. Sidorin, K. K. Sidorin, V. I. Pshenitsyn, and V. M. Zolotarev, "Study of the nature of a polished quartz-glass surface by ellipsometric and spectroscopic methods," *Optics and Spectroscopy* **52**(5), 852–857 (1982).
32. Y. Ikuta, S. Kikugawa, T. Kawahara, H. Mishiro, N. Shimodaira, and S. Yoshizawa, "New silica glass AQF for 157-nm lithography," in *Optical Microlithography XIII*, C. J. Proglor, ed., vol. 4000, pp. 1510–1514 (SPIE, 2000).
33. K. Kajihara, "Improvement of vacuum-ultraviolet transparency of silica glass by modification of point defects," *Journal of the Ceramic Society of Japan* **115**(2), 85–91 (2007).
34. G. H. Sigel, "Ultraviolet spectra of silicate glasses: A review of some experimental evidence," *Journal of Non-Crystalline Solids* **13**(3), 372–398 (1974).
35. N. Shimodaira, K. Saito, A. Ikushima, T. Kamihori, and S. Yoshizawa, "UV

- transmittance of fused silica glass influenced by thermal disorder,” vol. 4000, pp. p. 1553–1559 (SPIE, 2000).
36. H. Rawson, *Glass Science and Technology, Vol.3: Properties and Applications of Glass* (Elsevier Science, New York, NY, 1980).
  37. C. M. Smith and L. A. Moore, “Fused silica for 157-nm transmittance,” in *Emerging Lithographic Technologies III*, Y. Vladimirsky, ed., vol. 3676, pp. 834–841 (SPIE, 1999).
  38. Y. Ikuta, S. Kikugawa, T. Kawahara, H. Mishiro, K. Okada, K. Ochiai, K. Hino, T. Nakajima, M. Kawata, and S. Yoshizawa, “New modified silica glass for 157-nm lithography,” in *Photomask and Next-Generation Lithography Mask Technology VII*, H. Morimoto, ed., vol. 4066, pp. 564–570 (SPIE, 2000).
  39. D. Griscom, “The electronic structure of SiO<sub>2</sub>: A review of recent spectroscopic and theoretical advances,” *Journal of Non-Crystalline Solids* **24**(2), 155–234 (1977).
  40. V. Petrov and S. Stepanov, “Radiation characteristics of quartz glasses spectral radiating power,” *Teplofizika Vysokikh Temperatur* **13**, 335–345 (1975).
  41. V. Plotnichenko, V. Sokolov, and E. Dianov, “Hydroxyl groups in high-purity silica glass,” *Journal of Non-Crystalline Solids* **261**, 186–194 (2000).
  42. A. M. Efimov and V. G. Pogareva, “IR absorption spectra of vitreous silica and silicate glasses: The nature of bands in the 1300 to 5000 cm<sup>-1</sup> region,” *Chemical*

- Geology **229**(1-3), 198–217 (2006).
43. D. J. Griffiths, *Introduction to Electrodynamics*, 3<sup>rd</sup> edition (Prentice-Hall, Upper Saddle River, NJ, 1999).
  44. W. Rodney and R. Spindler, “Index of refraction of fused quartz for ultraviolet, visible, and infrared wavelengths,” *Journal of the Optical Society of America* **44**, 677–679 (1954).
  45. C. Tan and J. Arndt, “Temperature dependence of refractive index of glass SiO<sub>2</sub> in the infrared wavelength range,” *Journal of Physics and Chemistry of Solids* **61**, 1315–1320 (2000).
  46. L. Dombrovsky, “Quartz-fiber thermal insulation: infrared radiative properties and calculation of radiative-conductive heat transfer,” *Journal of Heat Transfer* **118**, 408–414 (1996).
  47. D. D. S. Meneses, G. Gruener, M. Malki, and P. Echegut, “Causal Voigt profile for modeling reflectivity spectra of glasses,” *Journal of Non-Crystalline Solids* **351**, 124–129 (2005).
  48. D. D. S. Meneses, M. Malki, and P. Echegut, “Structure and lattice dynamics of binary lead silicate glasses investigated by infrared spectroscopy,” *Journal of Non-Crystalline Solids* **352**, 769–776 (2006).
  49. S. Popova, T. Tolstykh, and V. Vorobev, “Optical characteristics of amorphous quartz in the 1400–200 cm<sup>-1</sup> region,” *Optics and Spectroscopy* **33**, 444–445 (1972).

50. H. R. Philipp, *Silicon dioxide (SiO<sub>2</sub>) glass*, in: E. D. Palik (Ed.), *Handbook of Optical Constants of Solids, Vol.I* (Academic Press, New York, NY, 1985 (p. 749)).
51. D. G. Drummond, “The infra-red absorption spectra of quartz and fused silica from 1 to 7.5  $\mu$  II - experimental results,” *Proceedings of the Royal Society of London. Series A, Mathematical and Physical Sciences* **153**(879), 328–339 (1936).
52. H. R. Philipp, “Optical transitions in crystalline and fused quartz,” *Solid State Communications* **4**, 73–75 (1966).
53. H. R. Philipp, “Optical properties of non-crystalline Si, SiO, SiO<sub>x</sub> and SiO<sub>2</sub>,” *The Journal of Physics and Chemistry of Solids* **32**, 1935–1945 (1971).
54. P. Lamy, “Optical constants of crystalline and fused quartz in the far ultraviolet,” *Applied Optics* **16**(8), 2212–2214 (1977).
55. “<http://www.tpdsci.com/Tpc/RIQtzFsd.php>,” .
56. C. Tan and J. Arndt, “Refractive index, optical dispersion, and group velocity of infrared wave in silica glass,” *Journal of Physics and Chemistry of Solids* **62**, 1087–1092 (2001).
57. C. Boeckner, “A method of obtaining the optical constants of metallicly reflecting substances in the infrared,” *Journal of the Optical Society of America* **19**, 7–15 (1929).
58. O. Girin, Y. Kondratev, and E. Raaben, “Optical constants and spectral mi-

- crocharacteristics of NaO<sub>2</sub>-SiO<sub>2</sub> glasses in the IR region of the spectrum,” *Optics and Spectroscopy* **29**, 397–403 (1970).
59. J. Wray and J. Neu, “Refractive Index of several glasses as a function of wavelength and temperature,” *Journal of the Optical Society of America* **59**, 774–776 (1969).
60. V. Zolotarev, “The optical constants of Amorphous SiO<sub>2</sub> and GeO<sub>2</sub> in the valence band region,” *Optics and Spectroscopy* **29**, 34–37 (1970).
61. I. Simon and H. McMahon, “Study of the structure of quartz, cristobalite, and vitreous silica by reflection in infrared,” *Journal of Chemical Physics* **21**, 23–30 (1953).
62. M. Herzberger and C. Salzberg, “Refractive indices of infrared optical materials and color correction of infrared lenses,” *Journal of the Optical of America* **52**, 420–427 (1962).
63. T. Yamamuro, S. Sato, T. Zenno, N. Takeyama, H. Matsuhara, I. Maeda, and Y. Matsueda, “Measurement of refractive indices of 20 optical materials at low temperatures,” *Optical Engineering* **45**(8), 083,401 (2006).
64. H. Bach and N. N. (Editors), *The Properties of Optical Glass* (Springer Verlag, 1998).
65. E. Beder, C. Bass, and W. Shackelford, “Transmittivity and absorption of fused quartz between 0.2 and 3.5  $\mu\text{m}$  from room temperature to 1500°C,” *Journal of*

- the American Ceramic Society **10**, 2263–2268 (1971).
66. D. Gillespie, A. Olsen, and L. Nichols, “Transmittance of optical materials at high temperatures in the 1- $\mu$  to 12- $\mu$  range,” *Applied Optics* **4**, 1488–1493 (1965).
  67. G. Calingaert, S. Heron, and R. Stair, “Sapphire and other new combustion-chamber window materials,” *S.A.E. Journal* **39**, 448–450 (1936).
  68. D. Heath and P. Sacher, “Effects of a simulated high-energy space environment on the ultraviolet transmittance of optical material between 1050 Å and 3000 Å,” *Applied Optics* **5**, 937–943 (1966).
  69. A. F. Grenis and M. J. Matkovich, “Blackbody reference for temperature above 1200 K. Study for design requirements,” AMRA-TR-65-02 pp. 1–18 (1965).
  70. G. V. Saidov and E. B. Bernstein, “Optical constants of surface layer of fused quartz in the 900-1300  $\text{cm}^{-1}$  range,” *Fizika i Khimiya Stekla* **8**(1), 75–81 (1982).
  71. A. M. Efimov, “Dispersion of optical constants of vitreous solids,” Ph.D. thesis, Vavilov State Optical Institute, Leningrad.
  72. R. K. Bogens and A. G. Zhukov, “The optical constants of fused quartz in the far infrared,” *Journal of Applied Spectroscopy* **25**(1), 54–55 (1966).
  73. T. J. Parker, J. E. Ford, and W. G. Chambers, “The optical constants of pure fused quartz in the far-infrared,” *Infrared Physics* **18**, 215–219 (1978).
  74. A. P. Zhilinskii, A. P. Gorchakov, T. S. Egorova, and N. A. Miskinova, “Optical characteristics of fused quartz in the far IR range,” *Optics and Spectroscopy*

- 62**(6), 783–784 (1987).
75. W. Bagdade and R. Stolen, “Far infrared absorption in fused quartz and soft glass,” *Journal of Physics and Chemistry of Solids* **29**(11), 2001–2008 (1968).
76. G.-L. Tan, M. F. Lemon, and R. H. French, “Optical properties and London dispersion forces of amorphous silica determined by vacuum ultraviolet spectroscopy and spectroscopic ellipsometry,” *Journal of the American Ceramic Society* **86**(11), 1885–1892 (2003).
77. P. T. T. Wong and E. Whalley, “Infrared and Raman spectra of glasses. Part 2. Far infrared spectrum of vitreous silica in the range 100 - 15  $\text{cm}^{-1}$ ,” *Discussions of the Faraday Society* **50**, 94–102 (1970).
78. R. K. Mamedov, G. M. Mansurov, and N. I. Dubovikov, “Optical constants of quartz glass in the IR range,” *Optiko-Mekhanicheskaya Promyshlennost* [Optical and Mechanical Industry (Sov. J. Opt. Technol., vol. 49, p.256 (1982))] **4**, 56 (1982).
79. M. Miler, “Infrared absorption of glassy silicon dioxide,” *Czechoslovak Journal of Physics* **18**(3), 354–362 (1968).

## List of Tables

- 1 Summary of the experimental data reporting the complex index of refraction of silica glass at room temperature (RT: room temperature). 33
- 2 Parameters used to interpolate the refractive index  $n_\lambda$  and absorption index  $k_\lambda$  of silica glass by using formulas (21) to (24). These parameters were obtained by fitting the equations to data of Popova *et al.*<sup>49</sup> . . . 35

## List of Figures

- 1 Real  $n_\lambda$  and imaginary  $k_\lambda$  parts of the complex refractive index of silica glass reported in the literature and summarized in Table 1. The solid curve (present study) was obtained with Equations (21) through (24) by using coefficients listed in Table 2. . . . . 36
- 2 Real  $n_\lambda$  and imaginary  $k_\lambda$  parts of the complex refractive index of silica glass between 30 nm and 1  $\mu\text{m}$  as reported in the literature and summarized in Table 1. . . . . 37
- 3 Real  $n_\lambda$  and imaginary  $k_\lambda$  parts of the complex refractive index of silica glass between 1  $\mu\text{m}$  and 15  $\mu\text{m}$  as reported in the literature and summarized in Table 1. The solid curve (present study) was obtained with Equations (21) through (24) by using coefficients listed in Table 2. 38

4	Real $n_\lambda$ and imaginary $k_\lambda$ parts of the complex refractive index of silica glass between 15 $\mu\text{m}$ and 100 $\mu\text{m}$ as reported in the literature and summarized in Table 1. The solid curve (present study) was obtained with Equations (21) through (24) by using coefficients listed in Table 2.	39
5	Real $n_\lambda$ and imaginary $k_\lambda$ parts of the complex refractive index of silica glass between 100 $\mu\text{m}$ and 1000 $\mu\text{m}$ as reported in the literature and summarized in Table 1. . . . .	40
6	Residuals between experimental <sup>49</sup> and predicted values of $n_\lambda$ and $k_\lambda$ . The predicted values are based on the Equation (21) through (24) with coefficients listed in Table 2. . . . .	41
7	Residuals between the experimental data on the refractive index and absorption index and values predicted in this work by using formulas (21) to (24) along with coefficients listed in Table 2. . . . .	42

Table 1. Summary of the experimental data reporting the complex index of refraction of silica glass at room temperature (RT: room temperature).

Ref.	Wavelength range ( $\mu\text{m}$ )	Measurement method	Reported data	Temp.	Sample thickness	Type	Comments
11	7.14 - 25	Reflection, transmission, Kramers-Krönig relation	n, k	RT	N/A	I	Vitreosil $\text{\textcircled{B}}$
12	2 - 500	Reflection, Kramers-Krönig method	R, n, k	300, 200, 100 and 10K	N/A	III	Suprasil, UV grade synthetic fused $\text{SiO}_2$
13	7-300	Transmission	n, k	RT	N/A	N/A	
15	110 - 550	Interferometric	T, n, $\kappa$	RT	2.1409 mm	I	Infrasil (low $\text{H}_2\text{O}$ )
16	3 - 6.7	Interferometric	n, T	RT	of $5 \times 10^{-4}$ 0.23 mm	III	Suprasil 2 $\sim 1000$ ppm OH-content
23	0.21 - 3.71	Minimum deviation method	n	20°C	N/A	III	Corning code 7940, Dynasil high-purity synthetic $\text{SiO}_2$ glass and GE type 151
25	0.80 - 2.60	k from Eq.(14)	T	298 K	1.6 mm	N/A	
26	0.19 - 0.42	k from Eq.(14)	T	298 K	2 mm	N/A	
27	0.05 - 0.7	Reflection and Kramers-Krönig	n, $\epsilon''$	RT	N/A	III	Suprasil (UV grade)
28	7.19 - 9.06	Interferometric	n, T, R	RT	0.1956 mm	IV	Suprasil W2
29	0.2 - 3	Reflection and transmission	n, k, R, T	24°C	N/A	N/A	
30	16.7 - 25	Reflection	R, n, k	RT	N/A	N/A	
44	0.35 - 3.51	Minimum deviation method	n	24°C	N/A	N/A	Samples from General Electric, Heraeus, Nieder Fused Quartz, and Corning Glass Works
45	1.44 - 4.77	Interferometric	n, T	23.5 - 481°C	0.1994 mm	IV	Suprasil W2
49	7.14 - 50	Reflection	n, k	RT	N/A	II	KU and KI
50	0.0006 - 500	Kramers-Krönig relation	n, k			IV	Impurity didn't exceed 0.007% compilation of data
51	1.00 - 7.5	Transmission	T, $\kappa$	RT	N/A	N/A	
54	0.10 - 0.16	Reflection and Kramers-Krönig	n, k	RT	5 $\mu\text{m}$ to 3.06 m	N/A	Samples produced by Electro-Quartz
56	1.35 - 4.85	Interferometric	n, T	23.5°C	0.2345 mm	IV	Suprasil W2
57	8.13 - 9.63	Reflection	R, n, k	RT	N/A	N/A	
58	7.84 - 12.9	Reflection	n, k	RT	N/A	N/A	

Ref.	Wavelength range ( $\mu\text{m}$ )	Measurement method	Reported data	Temp.	Sample thickness	Type	Comments
59	0.23 - 3.37	Minimum deviation method	n	26, 471 and 828°C	N/A	III	Corning 7940
60	7.14 - 11.11	Reflection, Transmission, and Kramers-Krönig relation	n, k	RT	N/A	II III IV	KU, KV KI
61	7.14 - 14.29	Reflection	R, k	RT	N/A	I	Infrasil
62	0.5 - 4.5	Minimum deviation	n	RT	N/A	N/A	Sample having low water content supplied by General Electric Company
63	0.37, 0.44, 0.55, 1.01, and 1.53	Minimum deviation	n	294, 240, 180 and 120 K	N/A	N/A	
64	0.06-40	Transmission	n, k	RT	N/A	N/A	
65	0.2 - 3.5	Transmission	k, T	RT - 1500°C	0.953 mm	I, III	GE IR Type 105, GE UV Type 151, and Corning Vycor IR Glass No. 7905
66	2.00 - 6.00	k from Eq.(14)	T	25 and 400°C	2.8 mm	I	
67	0.31 - 3.97	k from Eq.(14)	T	RT	5.45 mm	N/A	
68	0.16 - 0.30	k from Eq.(14)	T	RT	2.04-3.29 mm	III	Corning code 7940 and Dynasil
69	1.00 - 4.62	k from Eq.(14)	T	RT	3.18 mm		
70	7.69 - 11.11	Reflection, and Kramers-Krönig	n, k	RT	1.0 mm	II	KU, Optical Grade Fused Quartz
71	7.41 - 50	Reflection, and dispersion analysis <sup>24</sup>	n, k	RT	N/A	IV	KI
72	60 - 560	Transmission, and reflection	R, n, k	RT	0.258, 1.05, 2.03, 4.07, 12.35, 12.35, and 25 mm	N/A	$\text{Al}_2\text{O}_3 \leq 4.0 \times 10^{-3} \%$ , $\text{Fe}_2\text{O}_3 \leq 4.0 \times 10^{-3} \%$ , $\text{CaO} \leq 2.0 \times 10^{-3} \%$ , $\text{Na}_2\text{O} \leq 1.0 \times 10^{-3} \%$ , $\text{CuO}, \text{TiO}_2, \text{mgO}, \text{Mn}_3\text{O}_4 < 0.001 \%$
73	83.3 - 500	Transmission	n, $\kappa$	300 K	1.340 $\pm$ 0.001 mm	N/A	optically polished
74	50 - 1000	Reflection and transmission	n, k	RT	N/A	N/A	impurity $\leq 3 \times 10^{-5}$
75	100 - 1000	Transmission	$\kappa$	RT	N/A	III	GE type 101 and type 106
76	0.029 - 1.77	Transmission, Reflection and Kramers-Krönig	T, R, n, k	RT	N/A		Suprasil I
77	100 - 667	Transmission	$\kappa$	100 and 300K			GE type 101
78	7.69-11.1	Internal reflection and Kramers-Krönig	n, k	RT	N/A	III	KU-1 glass, broken surface
79	2 - 35	Reflection and Kramers-Krönig	T, R, n, k	RT	N/A	N/A	

Table 2. Parameters used to interpolate the refractive index  $n_\lambda$  and absorption index  $k_\lambda$  of silica glass by using formulas (21) to (24). These parameters were obtained by fitting the equations to data of Popova *et al.*<sup>49</sup>

$j$	$\alpha_j$	$\eta_{0j}$	$\sigma_j$
1	3.7998	1089.7	31.454
2	0.46089	1187.7	100.46
3	1.2520	797.78	91.601
4	7.8147	1058.2	63.153
5	1.0313	446.13	275.111
6	5.3757	443.00	45.220
7	6.3305	465.80	22.680
8	1.2948	1026.7	232.14

$$\epsilon_\infty=2.1232$$

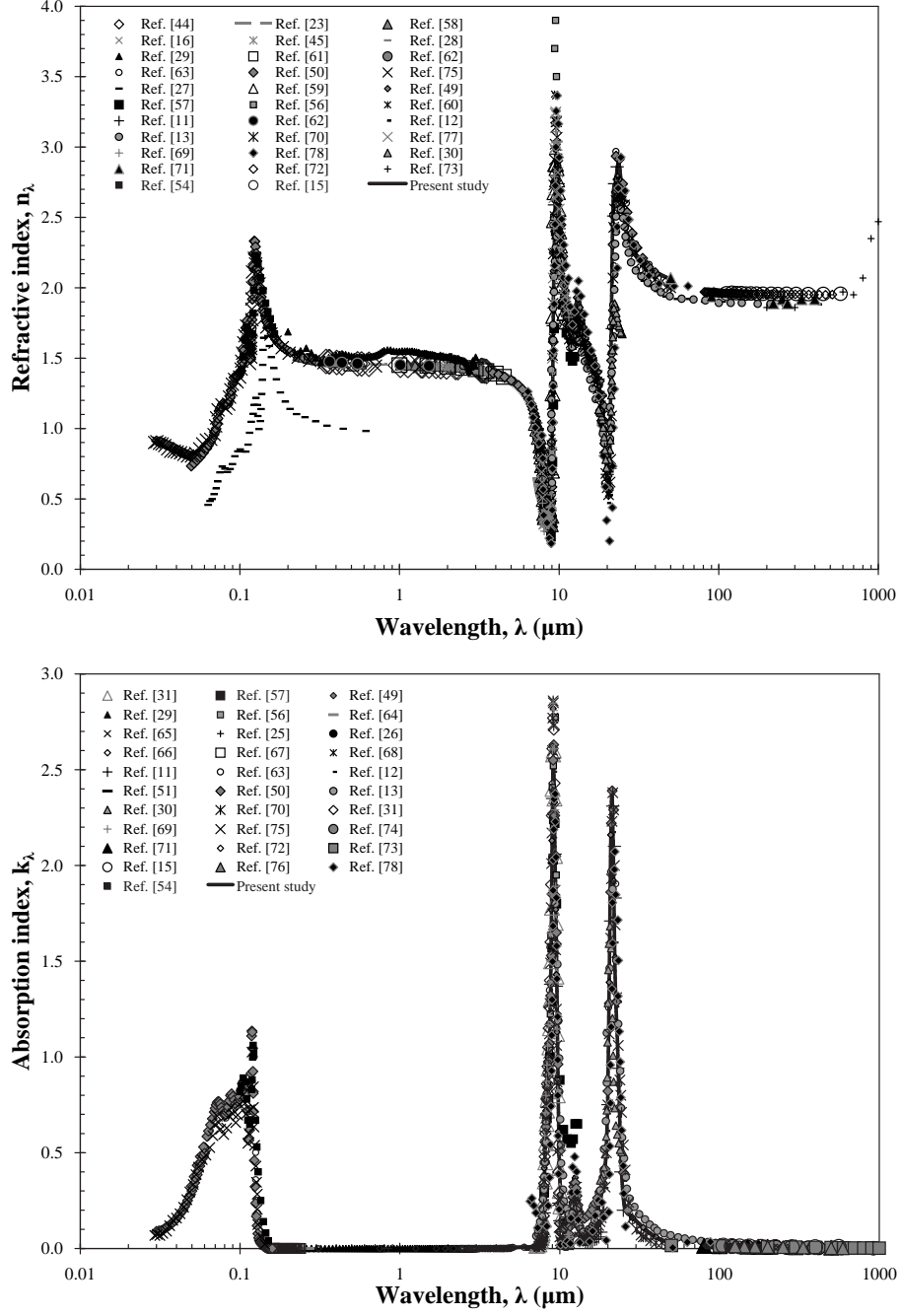


Fig. 1. Real  $n_\lambda$  and imaginary  $k_\lambda$  parts of the complex refractive index of silica glass reported in the literature and summarized in Table 1. The solid curve (present study) was obtained with Equations (21) through (24) by using coefficients listed in Table 2.

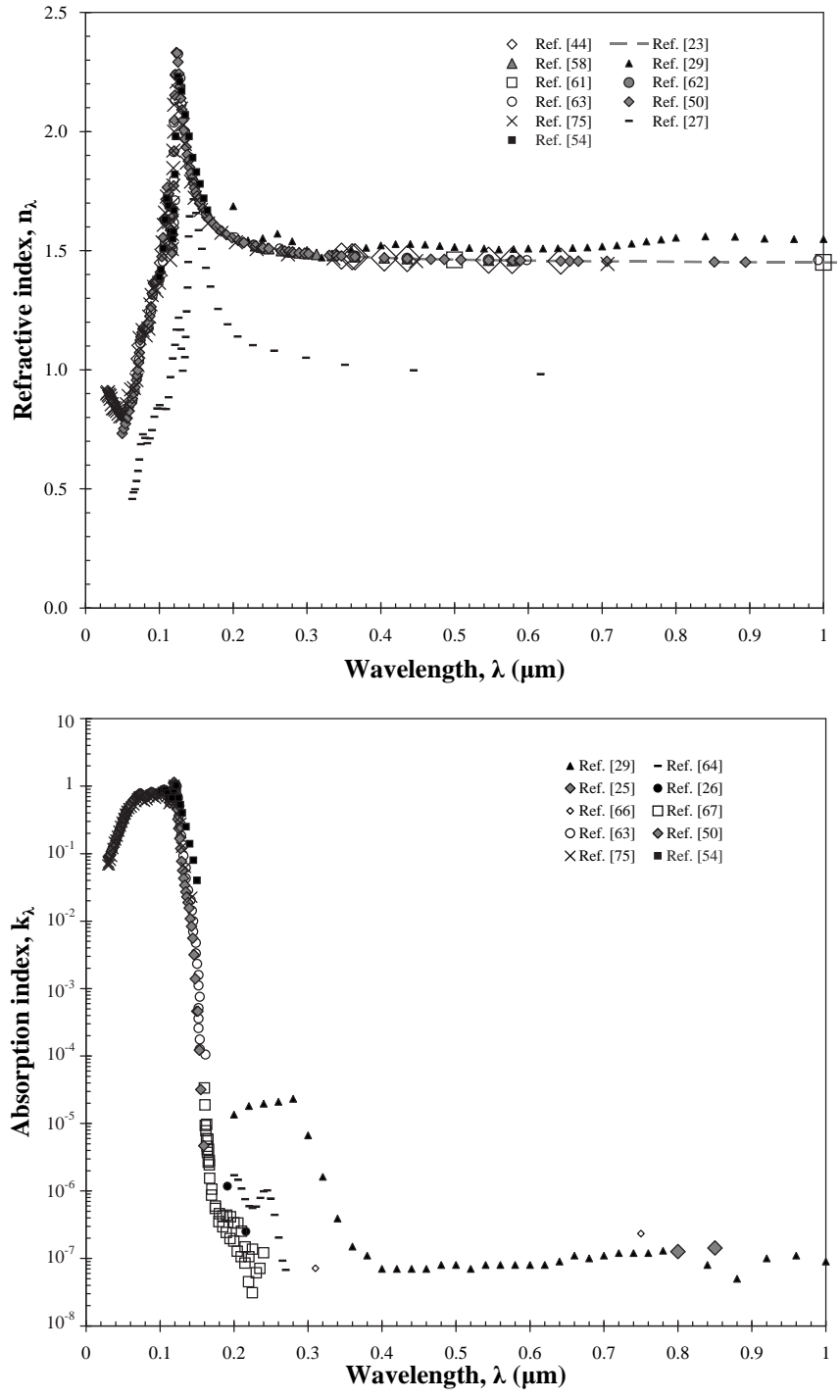


Fig. 2. Real  $n_\lambda$  and imaginary  $k_\lambda$  parts of the complex refractive index of silica glass between 30 nm and 1  $\mu\text{m}$  as reported in the literature and summarized in Table 1.

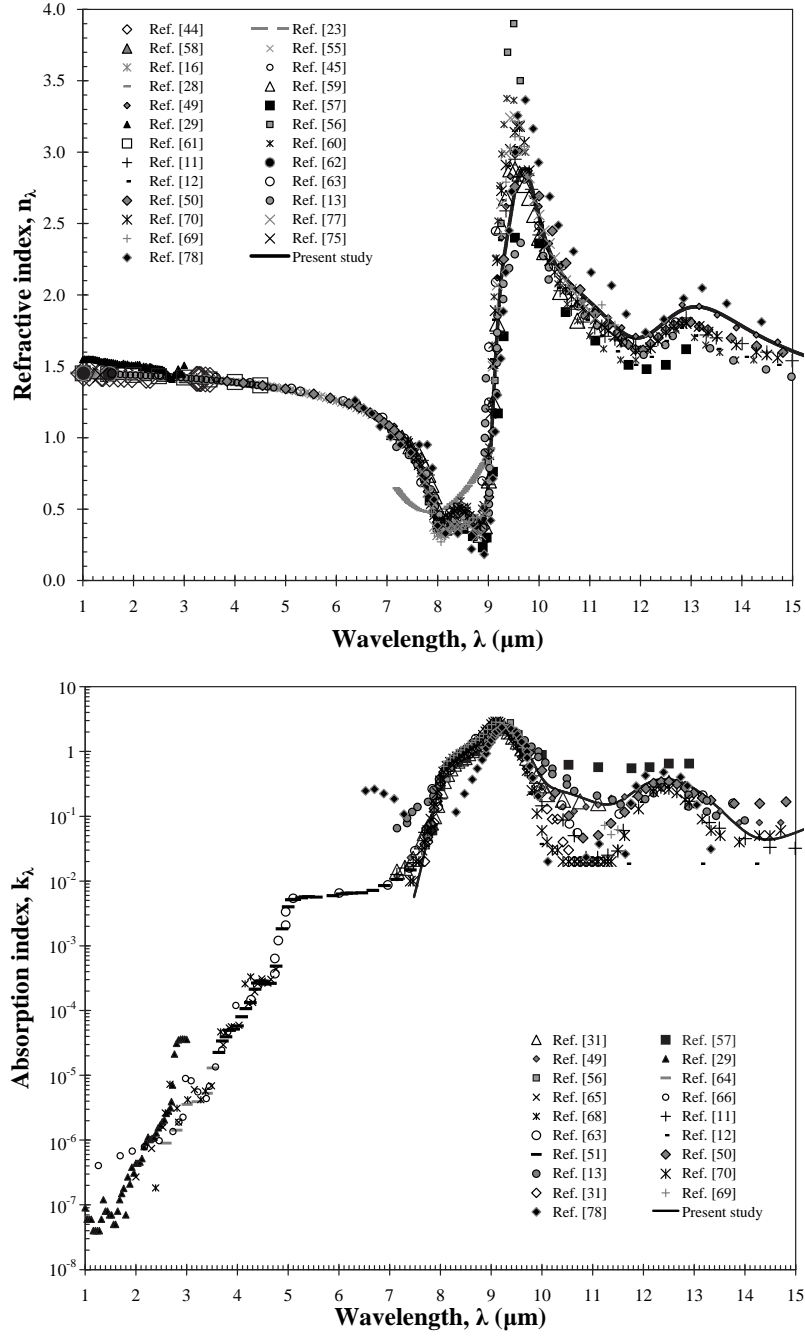


Fig. 3. Real  $n_\lambda$  and imaginary  $k_\lambda$  parts of the complex refractive index of silica glass between 1  $\mu\text{m}$  and 15  $\mu\text{m}$  as reported in the literature and summarized in Table 1. The solid curve (present study) was obtained with Equations (21) through (24) by using coefficients listed in Table 2.

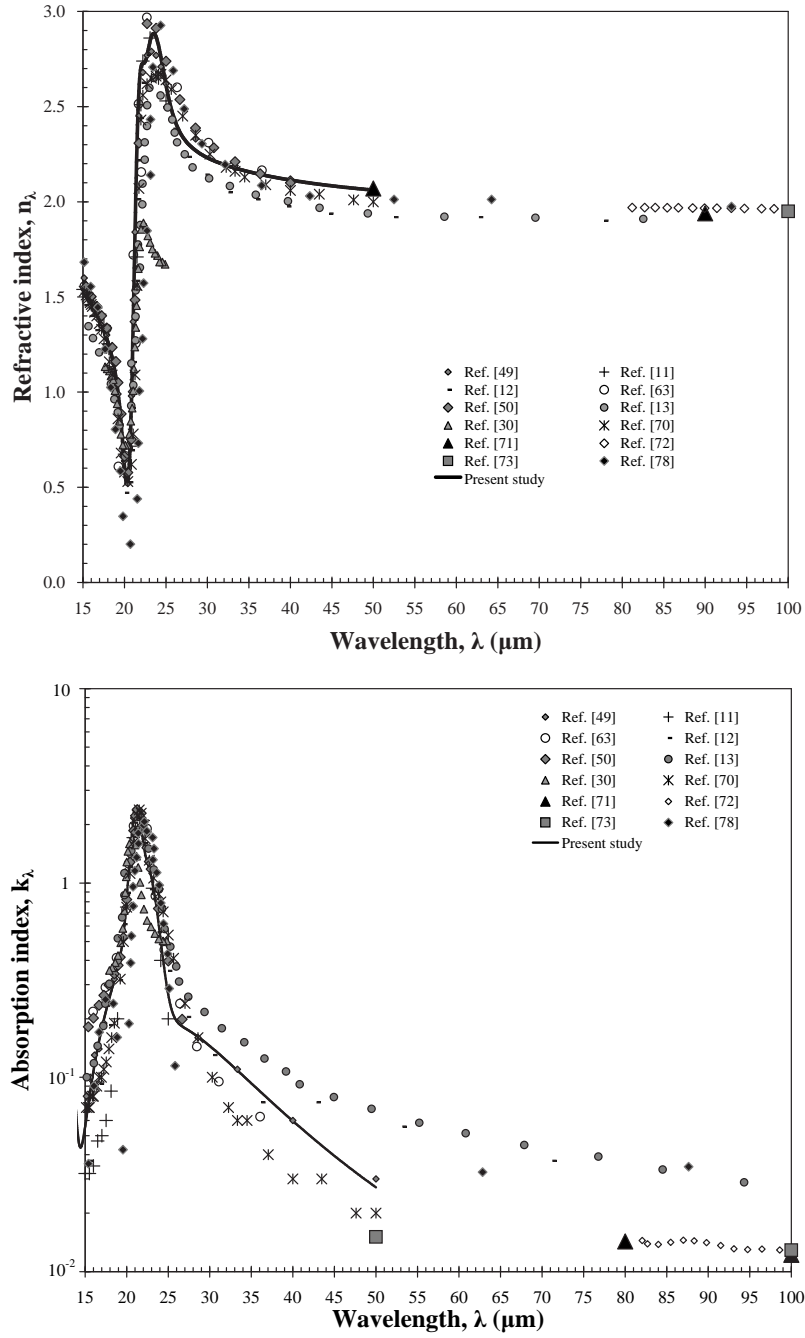


Fig. 4. Real  $n_\lambda$  and imaginary  $k_\lambda$  parts of the complex refractive index of silica glass between  $15 \mu\text{m}$  and  $100 \mu\text{m}$  as reported in the literature and summarized in Table 1. The solid curve (present study) was obtained with Equations (21) through (24) by using coefficients listed in Table 2.

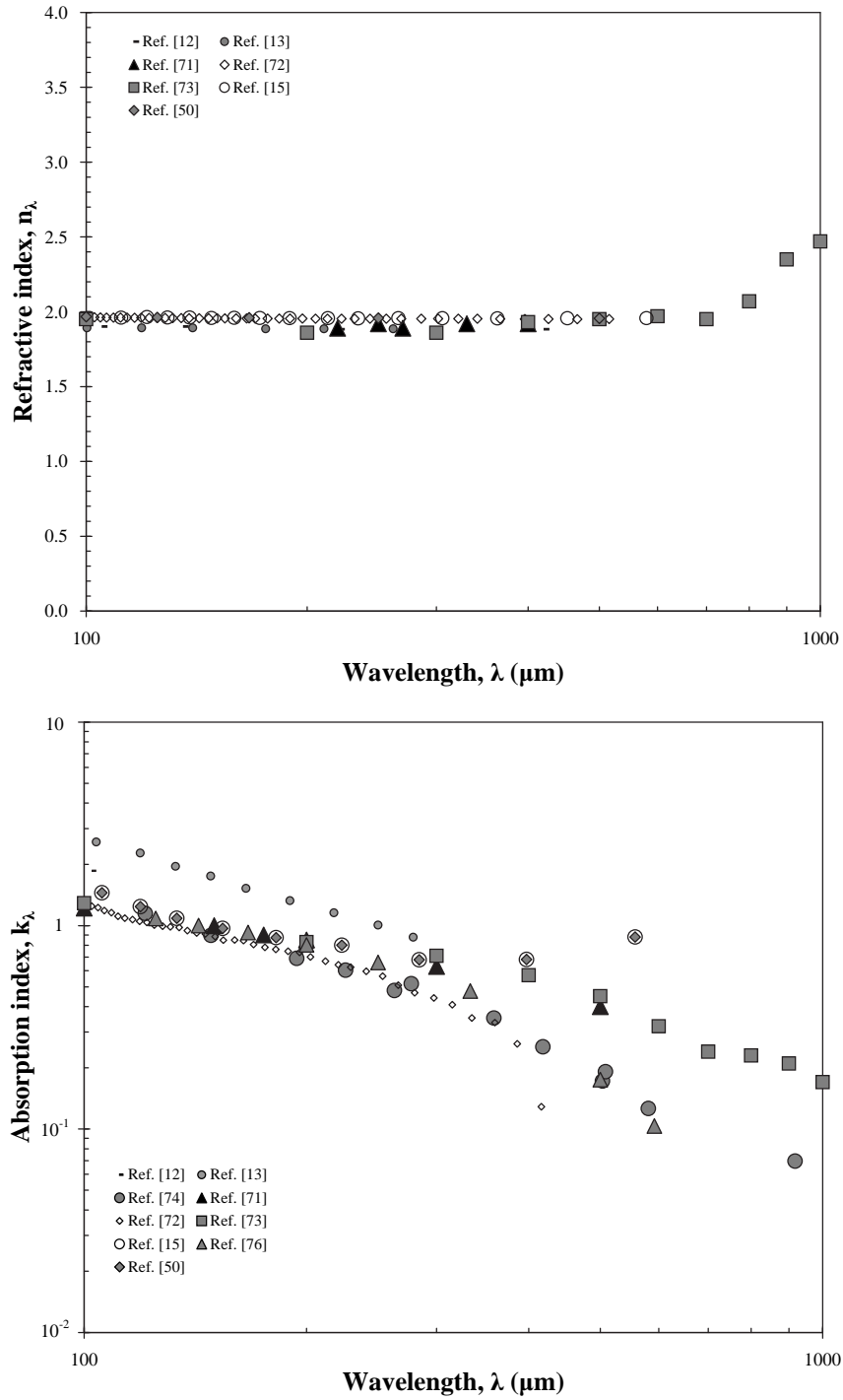


Fig. 5. Real  $n_\lambda$  and imaginary  $k_\lambda$  parts of the complex refractive index of silica glass between 100  $\mu\text{m}$  and 1000  $\mu\text{m}$  as reported in the literature and summarized in Table 1.

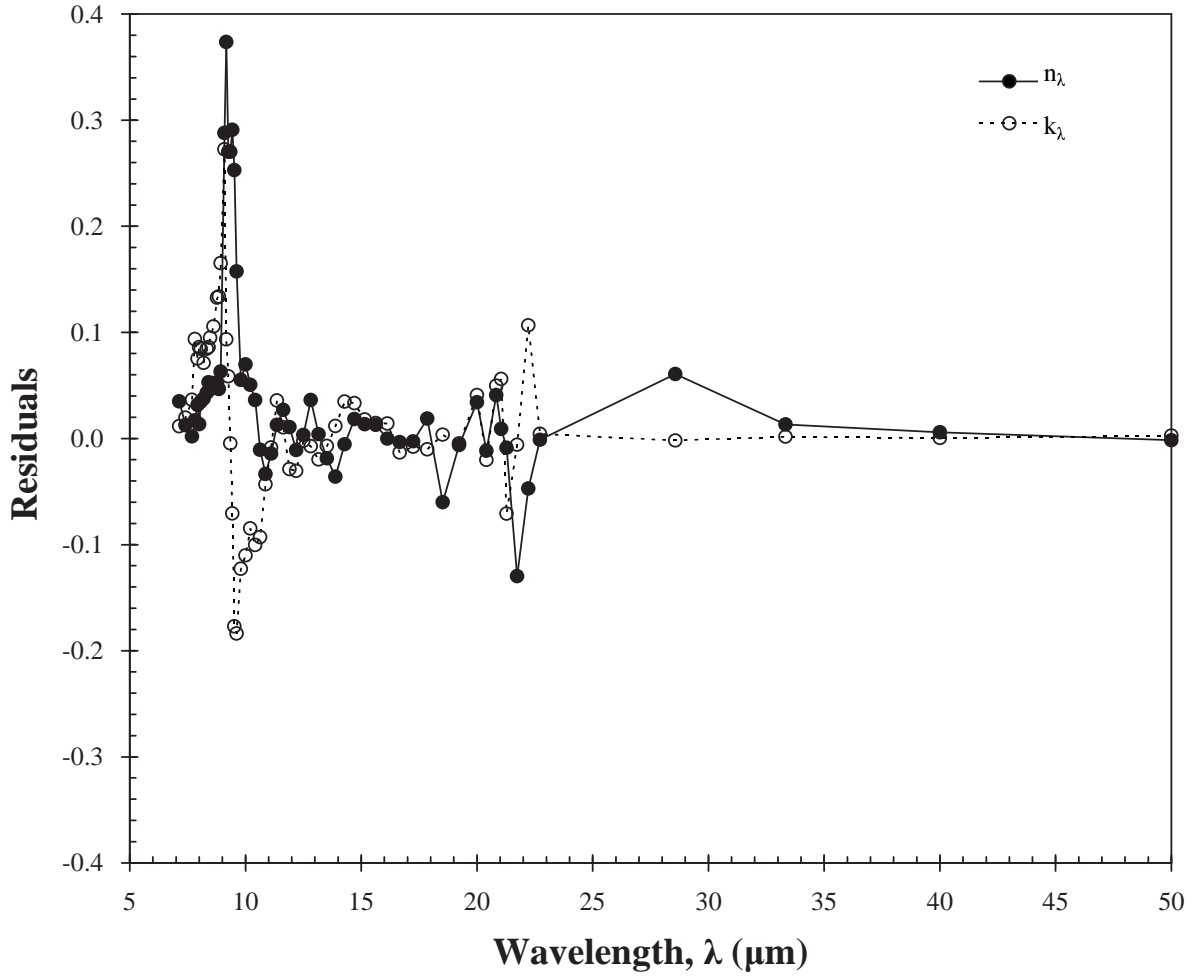


Fig. 6. Residuals between experimental<sup>49</sup> and predicted values of  $n_\lambda$  and  $k_\lambda$ .

The predicted values are based on the Equation (21) through (24) with coefficients listed in Table 2.

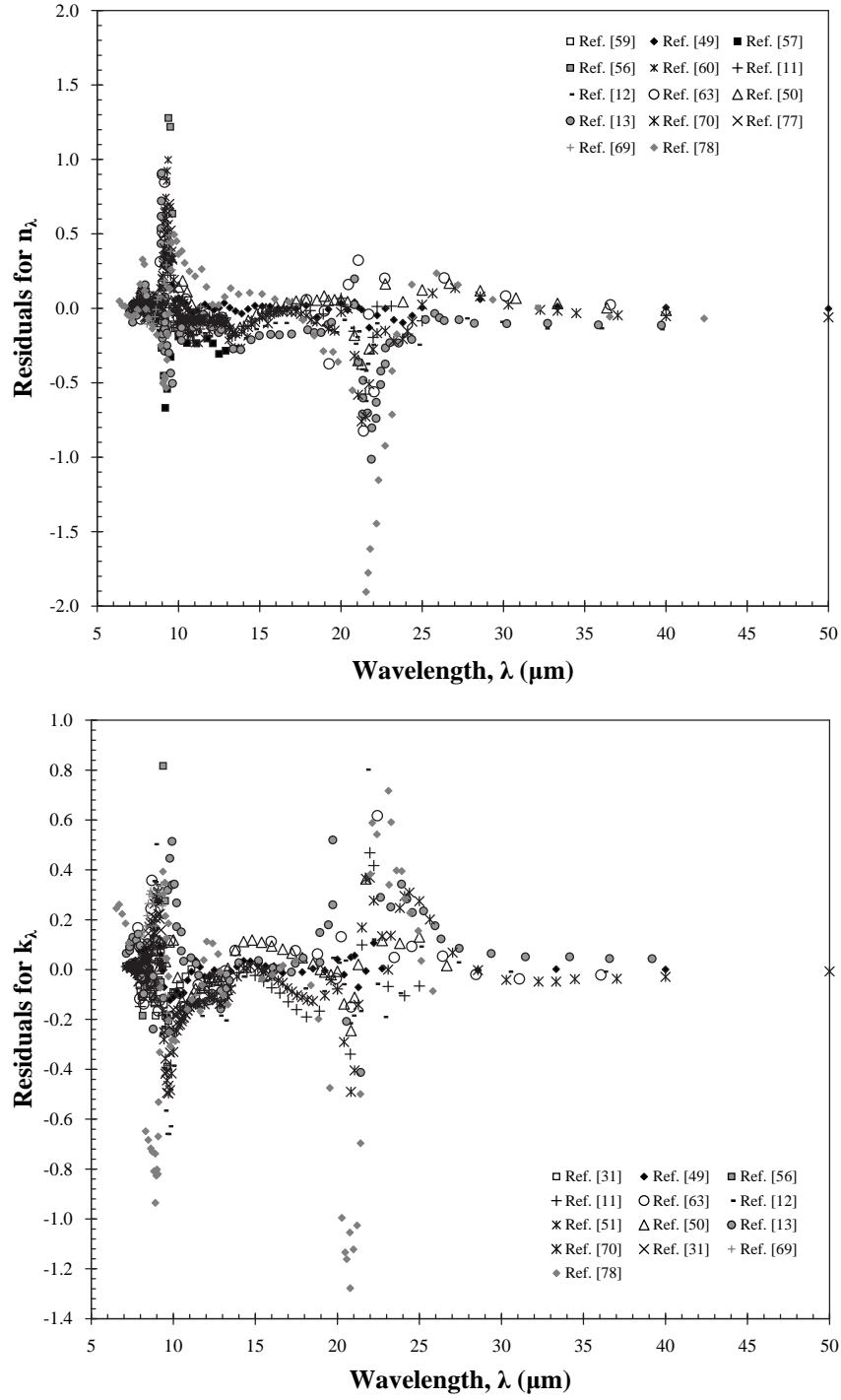


Fig. 7. Residuals between the experimental data on the refractive index and absorption index and values predicted in this work by using formulas (21) to (24) along with coefficients listed in Table 2.